

Proton Scattering from Even Samarium Isotopes*

P. STOLER, M. SLAGOWITZ, W. MAKOFKSKE, AND T. KRUSE

Department of Physics, Rutgers, The State University, New Brunswick, New Jersey

(Received 15 July 1966; revised manuscript received 7 September 1966)

Differential cross sections have been taken of 16-MeV protons elastically and inelastically scattered from even samarium isotopes. The behavior of the angular distributions exhibits marked change as the transition from the spherical vibrational nuclei to the deformed rotational nuclei is made. Results compare well with predictions of coupled channel calculations.

I. INTRODUCTION

IN recent years, coupled channel calculations have become increasingly popular in describing certain types of nuclear scattering and reactions. Extensive calculations have been carried out for scattering particles from nuclei which exhibit vibrational and rotational characteristics.¹⁻³

Such calculations utilize the optical-model approach, with the added feature that the nuclear radius R is assumed to depend upon angles θ and ϕ , with respect to a body-fixed set of coordinate axes: $R=R(\theta, \phi)$. The optical potential between nucleus and projectile is a function of R , and hence of θ and ϕ , i.e., $V=V(\theta, \phi)$. This potential can couple incident partial waves with orbital angular momentum l , $\psi_l^i(\theta, \phi)$, with scattered partial waves of orbital angular momentum l' , $\psi_{l'}^f(\theta, \phi)$ through the matrix elements $\langle \psi_{l'}^f(\theta, \phi) | V(\theta, \phi) | \psi_l^i(\theta, \phi) \rangle$. Because of conservation of angular momentum, the nuclei must take up the difference in angular momentum between initial and final channel by going into a final vibrational or rotational excited state. In addition, the outgoing channels may couple with each other. The differential cross sections of the elastic scattering and inelastic scattering which leave the target nucleus in excited rotational or vibrational states are then computed.

For nuclei with rotational properties, the adiabatic approximation has been quite useful in facilitating these computations.^{4,5} In particular, calculations for proton scattering from rotational and vibrational nuclei have been carried out by Tamura⁶ and Barrett.⁷

Recently, a review by Tamura⁸ has been published in which extensive calculations have been carried out. Comparison of theory with existing vibrational data⁹⁻¹¹ appears good. Rotational data are more difficult to

compile because in the regions of permanently deformed nuclei, the rotational levels lie very low and inelastic events to these levels are difficult to resolve from the much more numerous elastic events. Comparison has been made with the only available proton data by Lieber and Whitten.¹²

In this review, Tamura has made a direct comparison of expected results for rotational and vibrational targets. Here, the same Z and A are chosen for each, and the only difference between the two nuclei is that in one case the nucleus is assumed to have a spherical ground state with vibrational excited levels, and in the other, the nucleus is assumed to have a deformed ground state with rotational excited levels. The results are reproduced in Fig. 1.

In Fig. 1(B) the solid curves give the elastic and inelastic scattering cross sections to the first two rotational states of a permanently deformed nucleus specified in the caption. The value of β_2 , the deformation parameter used, is 0.32. The dashed curves are for a hypothetical spherical nucleus, with the same A and Z , having vibrational states. The 0^+ curve represents elastic scattering; the 2^+ represents inelastic scattering leaving the nucleus in the one-quadrupole-phonon 2^+ state; and the 4^+ represents inelastic scattering leaving the nucleus in the two-quadrupole-phonon 4^+ state. In this case, β_2 for the transitions between states is chosen as 0.20, a value close to that found in many vibrational

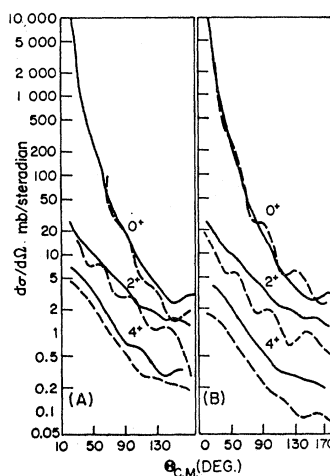


FIG. 1. Scattering cross sections of 17.5-MeV protons by a nucleus with $A=156$ and $Z=64$. Solid lines are for deformed nucleus and dashed lines are for vibrational nucleus. Figure 1(A) and 1(B) differ only in β values for the vibrators; there are obvious plotting errors in the lower two curves of Fig. 1(A). The lowest dashed curve should be solid and vice versa. From Ref. 8.

* Partially supported by the National Science Foundation.

¹ B. Buck *et al.*, *Phil. Mag.* **5**, 1181 (1960).

² B. Buck, A. P. Stamp, and P. E. Hodgson, *Phil. Mag.* **8**, 1805 (1963).

³ T. Tamura, *Phys. Letters* **9**, 334 (1964).

⁴ S. I. Drozdov, *Zh. Eksperim. i Teor. Fiz.* **28**, 734 (1955) [English transl.: *Soviet Phys.—JETP* **1**, 588 (1955)].

⁵ R. C. Barrett, *Nucl. Phys.* **51**, 27 (1964).

⁶ T. Tamura, *Phys. Letters* **12**, 121 (1964).

⁷ R. C. Barrett, *Phys. Rev. Letters* **14**, 115 (1965).

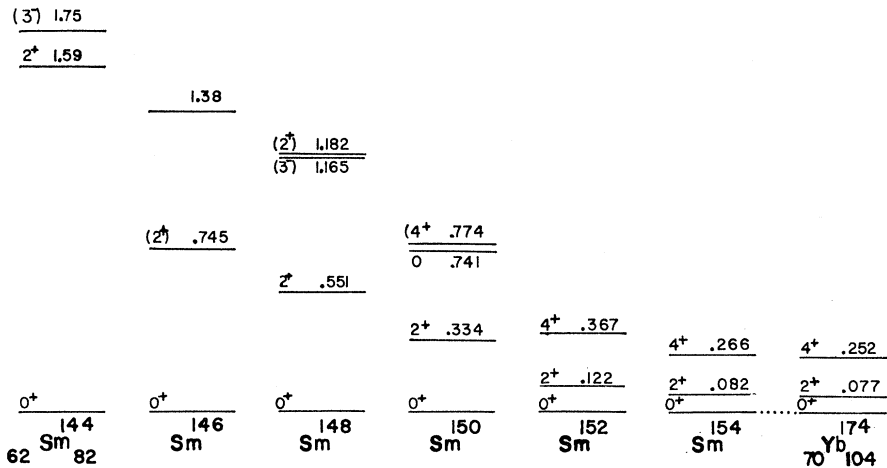
⁸ T. Tamura, *Rev. Mod. Phys.* **37**, 679 (1965).

⁹ T. Tamura, *Rev. Mod. Phys.* **37**, 697 (1965).

¹⁰ M. Sakai and T. Tamura, *Phys. Letters* **10**, 323 (1964).

¹¹ G. C. Pramila *et al.*, *Nucl. Phys.* **61**, 448 (1965).

¹² A. Lieber and C. A. Whitten, *Phys. Rev.* **132**, 258 (1963).



FIRST FEW ENERGY LEVELS OF EVEN-A SAMARIUM ISOTOPES

FIG. 2. First few energy levels of indicated isotopes demonstrating the transition from a vibrational spectrum to a rotational spectrum.

nuclei. Since cross sections of this type are expected to vary slowly with nuclear size and bombarding energy, qualitative comparison with these experimental results should be meaningful. [These calculations, however, assume no fourth-order deformations, as discussed by Barrett.⁷]

The nuclei which most closely fit the specifications of Fig. 1 are the even samarium isotopes. The lighter of these, ¹⁴⁴Sm-¹⁵⁰Sm, have the vibrational properties, and the heavier, ¹⁵²Sm-¹⁵⁴Sm, are across the sharp boundary between spherical and deformed ground states at A=150, and have good rotational characteristics. Figure 2 shows the first few energy levels of these isotopes, along with ¹⁷⁴Yb, which is well within the rotational region.

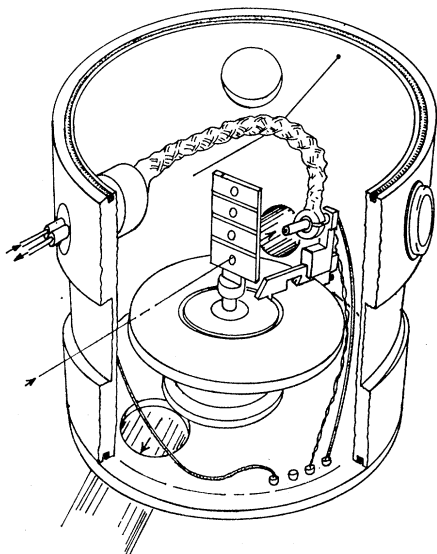


FIG. 3. Schematic diagram of chamber interior.

II. EXPERIMENT

Isotopically enriched samarium was obtained, in oxide form, from Oak Ridge National Laboratory. The oxides were thoroughly mixed with lanthanum metal powder, placed in a carbon crucible, and heated by

EXPERIMENTAL ARRANGEMENT

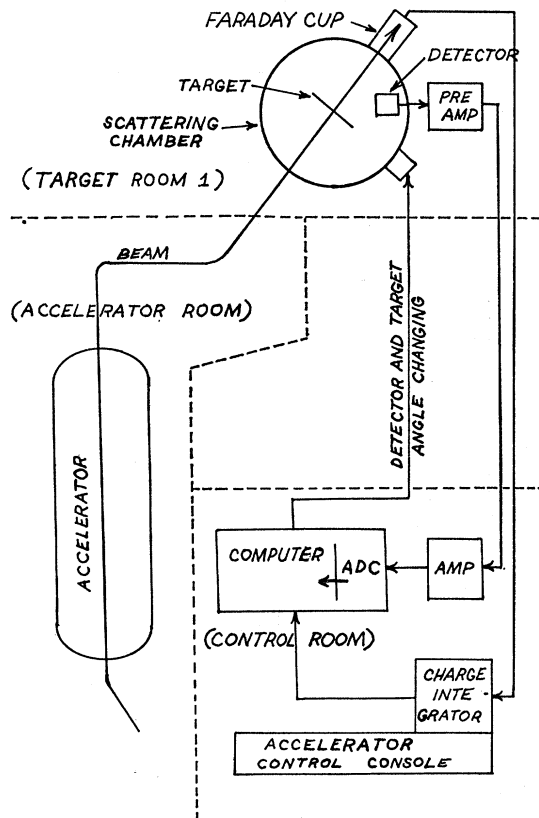


FIG. 4. Schematic view of experimental arrangement.

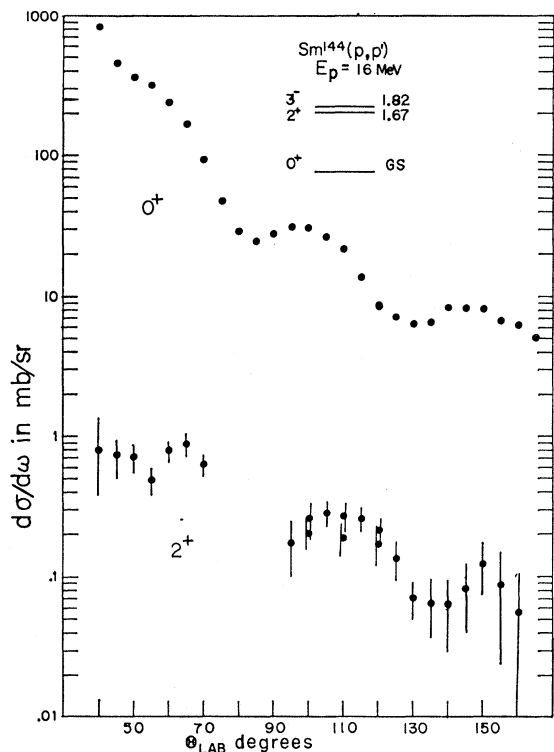


FIG. 5. Differential cross sections for $^{144}\text{Sm}(p,p)$ and $^{144}\text{Sm}(p,p')$.

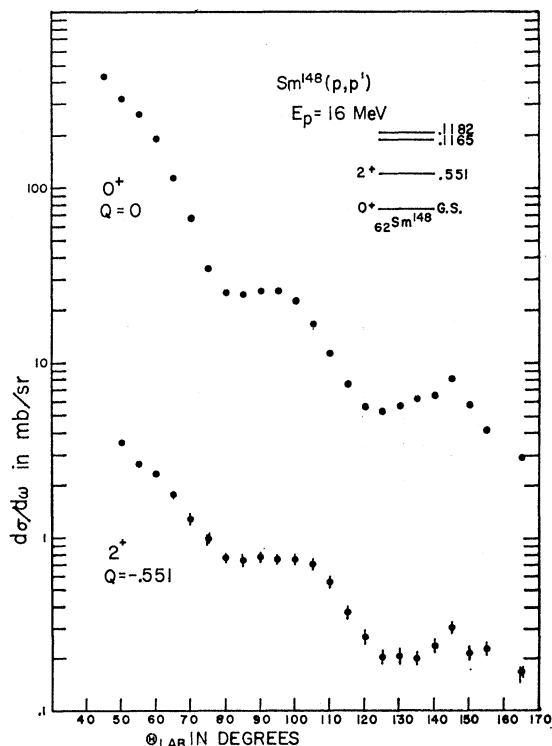


FIG. 6. Differential cross sections for $^{148}\text{Sm}(p,p)$ and $^{148}\text{Sm}(p,p')$.

electron bombardment. The lanthanum reduced the oxide, and the freed samarium differentially evaporated, in metallic form, onto thin carbon films. The typical target thickness was 100 or 200 $\mu\text{g}/\text{cm}^2$.

A 16-MeV proton beam was obtained using the Rutgers-Bell tandem Van de Graaff. This energy is well above the Coulomb barriers for the nuclei studied.

Lithium-drifted, 3-mm-deep silicon detectors were obtained from Technical Measurement Corporation. Since high-energy resolution is required to resolve the inelastic groups from the elastic group for the rotational nuclei, the detectors were cooled to a temperature about -100°C . This was accomplished by a flexible metallic braid which extended from the insulated detector housing to a copper liquid-nitrogen reservoir inside the chamber. The detector was mounted upon a turntable in the scattering chamber, and angle changing was accomplished automatically by computer control of driving motors geared to the turntable shaft. Figure 3 is a schematic cut-away of the scattering chamber interior.

Pulses from the detector were pre-amplified, further amplified and shaped, analyzed by an analog-to-digital converter,¹³ and accumulated in the memory of an SDS 910 computer; after each run memory content was

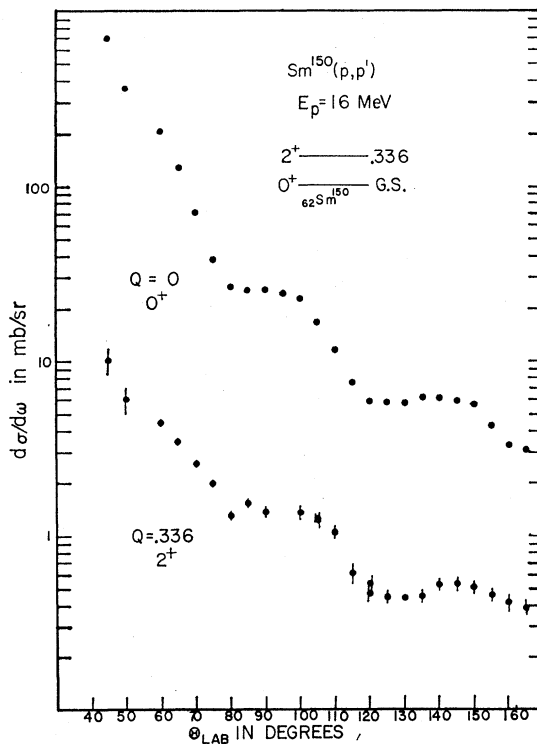
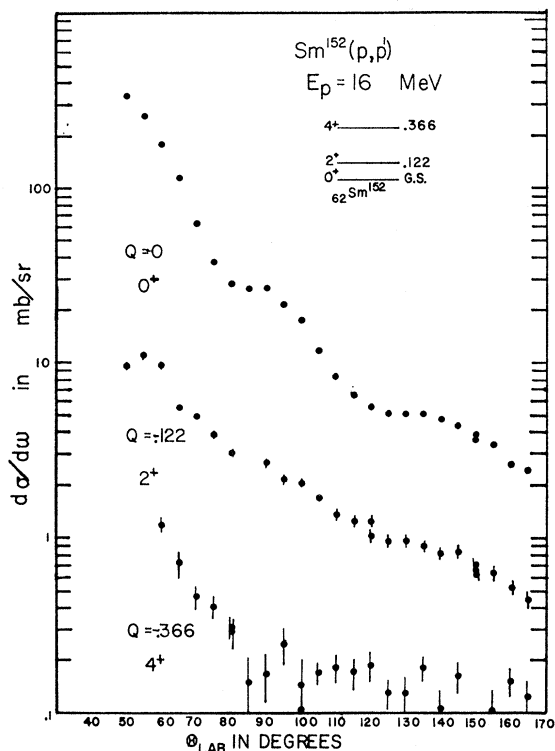
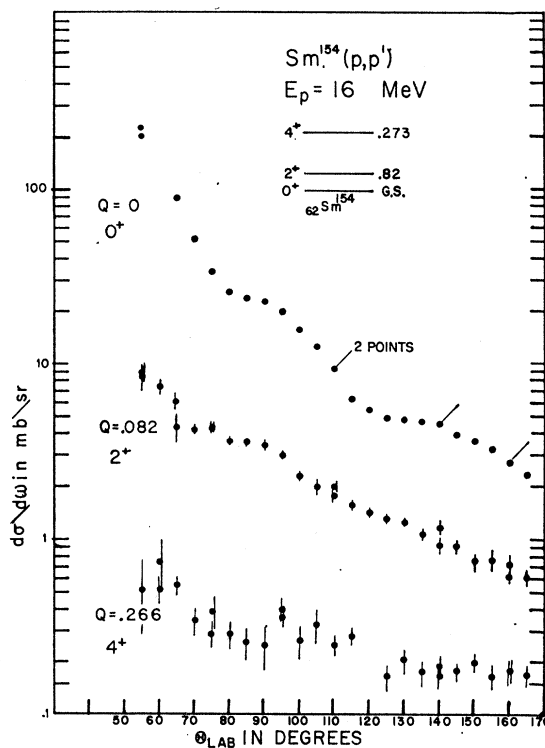


FIG. 7. Differential cross sections for $^{150}\text{Sm}(p,p)$ and $^{150}\text{Sm}(p,p')$.

¹³ E. A. Gere and G. L. Miller, in Proceedings of the Scintillation and Semiconductor Counter Symposium, Washington, D. C., 1966 (to be published in Proc. IEEE).

FIG. 8. Differential cross sections for $^{152}\text{Sm}(p,p)$ and $^{152}\text{Sm}(p,p')$.FIG. 9. Differential cross sections for $^{154}\text{Sm}(p,p)$ and $^{154}\text{Sm}(p,p')$.

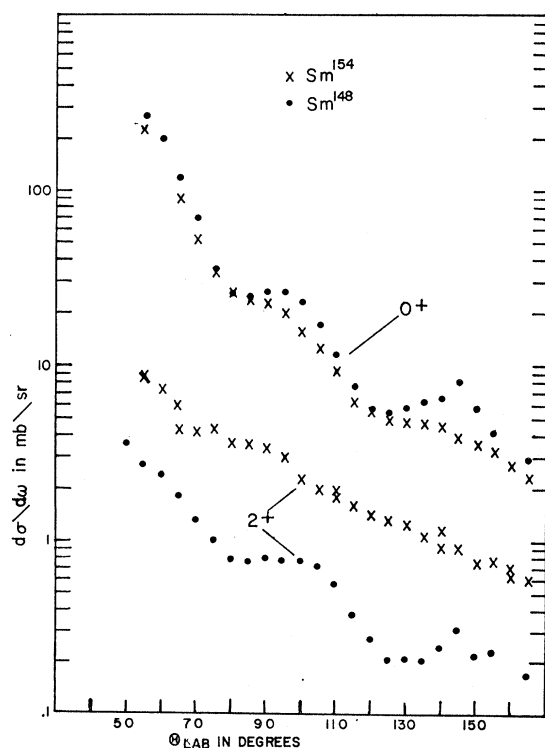
dumped onto magnetic tape.¹⁴ Well-resolved peaks were summed using computer light-pen routines,¹⁵ but partially resolved peaks were unfolded manually. The latter was required for ^{154}Sm since the peak corresponding to the inelastic scattering from the first excited state is only 82 keV from the elastic peak. The over-all resolution—full width at half-maximum—was generally about 25 to 40 keV.

A schematic of the experimental arrangement is shown in Fig. 4.

III. EXPERIMENTAL RESULTS

Of the nuclei studied, ^{144}Sm , ^{148}Sm , and ^{150}Sm are described as having spherical ground states and vibrational low-lying excited states, although ^{144}Sm has a closed neutron shell and the collective model is not completely applicable. ^{152}Sm and ^{154}Sm have permanently deformed ground states and rotational low-lying excited states.

Experimental results are shown in Figs. 5–9. (Errors shown are statistical in nature; systematic errors are believed to range to 5%.) A systematic variation with A in the shape of the angular distributions is apparent. In particular, the lower the energy of the first excited state, the more strongly it couples with the

FIG. 10. Superposition of elastic and inelastic differential cross sections for the vibrational nucleus ^{148}Sm and the rotational nucleus ^{154}Sm .

¹⁴ J. V. Kane and R. J. Spinrad, in Proceedings of the Conference on Utilization of Multiparameter Analyzers in Nuclear Physics, 1963 (unpublished).

¹⁵ J. F. Mollenauer, Nucleonics 23, 66 (1965).

ground state, and this causes a less pronounced diffraction pattern in the elastic and inelastic differential cross sections. The same coupling effect occurs for nuclei with larger values of β_2 . Also owing to the stronger coupling to the elastic scattering channel, the inelastic differential cross sections are greater for the nuclei with larger β_2 's and lower-lying collective levels. These considerations are illustrated in Fig. 10.

Figure 10 is a superposition of the elastic and the first-excited-state inelastic scattering cross sections for the vibrational nucleus ^{148}Sm and the rotational nucleus ^{154}Sm . From Coulomb excitation data, calculated values of β_2 for the $0^+ \rightarrow 2^+$ transitions are available: 0.16 for ^{148}Sm and 0.35 for ^{154}Sm .¹⁶ These values are close to those used by Tamura⁸ in the calculations shown in Fig. 1(B). Theory and experiment are in quite good agreement regarding the dependence of magnitude and shape of these differential cross sections on the character of the nuclear states involved. However, agreement between theory and experiment for the angular distribution of the inelastic scattering to the weakly excited 4^+ rotational states is not as satisfactory.

Figure 1(A) represents the same calculation as Fig. 1(B), except that in the vibrational case (dashed curve)

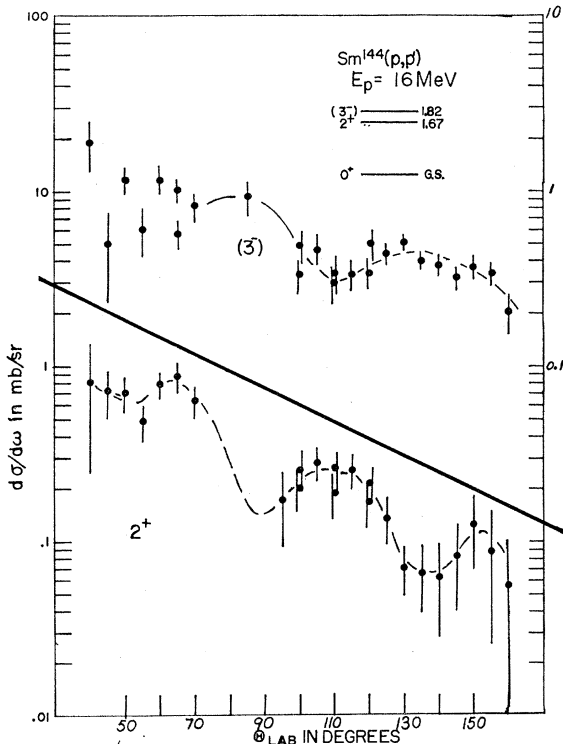


FIG. 11. Differential cross sections for $^{144}\text{Sm}(p,p')$. The left-hand scale corresponds to the bottom diagram while the right-hand scale corresponds to the top diagram.

¹⁶ P. Stelson and L. Grodzin, Nucl. Data **1A**, No. 1 (1965).

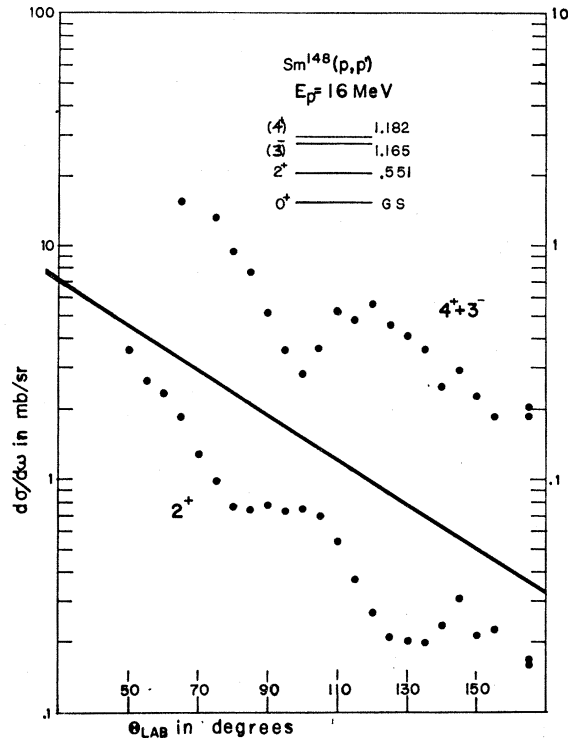


FIG. 12. Differential cross sections for $^{148}\text{Sm}(p,p')$. The left-hand scale corresponds to the bottom diagram while the right-hand scale corresponds to the top diagram.

the transition β_2 's were chosen to be 0.32—a value equal to that predicted for the rotational nucleus. The predicted angular distributions differ noticeably from the experimental curves.

Figure 11 shows the differential cross sections for the 2^+ and 3^- states in ^{144}Sm , and Fig. 12 those for the 2^+ and unresolved (4^+ and 3^-) doublet in ^{148}Sm . The 4^+ in the latter is presumed to be a two-phonon state, and to give a rather small contribution with respect to the one-phonon 3^- cross section. (This contribution has been shown to be about 10% at $\theta=115^\circ$, for 12-MeV protons.¹⁷) The distribution is therefore probably characteristic of the 3^- state. The maxima and minima are out of phase with the 2^+ distribution, as predicted.⁸ The general behavior of the corresponding angular distribution in Fig. 10 is similar.

We conclude that inelastic proton scattering provides a sensitive and reliable means of obtaining information about the strongly excited collective states of nuclei.

ACKNOWLEDGMENTS

We wish to thank Dr. T. Tamura for valuable discussions. We also wish to thank Dr. R. C. Barrett and Dr. G. M. Temmer for stimulating discussions.

¹⁷ R. Kenefick and R. K. Sheline, Phys. Rev. **133**, 25 (1963).